PCCP

Accepted Manuscript

ROYAL SOCIETY OF CHEMISTRY

www.rsc.org/pccp

Water as a morphological probe to study polymer-filler interfaces: an originalapplication of thermoporosimetry

Ahmedou Sidi [1,2], Jean-François Larché*[4], Pierre-Olivier Bussière[1,2], Jean-Luc Gardette [1,3], Sandrine Therias[1,3], Mohamed Baba [1,3,*]

[1] *Clermont Université, Université Blaise Pascal, Institut de Chimie de Clermont-Ferrand, BP 10448, F-63000 Clermont-Ferrand*

[2] *Clermont Université, ENSCCF, Institut de Chimie de Clermont-Ferrand, BP 10448, F-63000 Clermont-Ferrand*

[3] *CNRS, UMR 6296, ICCF, BP 80026, F-63171 Aubière*

[4]*Nexans Research Center, 29 rue du PréGaudry, 69353 Lyon Cedex 07*

[*]**Corresponding author:**

Mail :mohamed.baba@univ-bpclermont.fr

Phone : +33 (4) 73407161

Fax : +33 (4) 73407700

Key words: thermoporosimetry, water sorption, composites, interface

Abstract

This paper is devoted to the characterization of polymer-filler interfaces by thermoporosimetry using water as a probe. EVA filled with Aluminium hydroxide composites with high filler content for required fire properties have been studied. After water sorption at 90°C, the composites have been analyzed using thermoporosimetry with water as a morphological probe. This technique first allowed studying the influence of the filler content and specific surface area on the water uptake. The study with drying steps andtwo molecule probes (water and cyclohexane) have highlighted that water is confined at the interface and thus that thermoporosimetry is a powerful tool to characterize interfaces in EVA/ATH composites.

1. Introduction

Materials used in cable industry are in constant evolution and we face today an increasing need to use less hazardous material. A good example of this trend, pushed by environmental and safety reasons is the emergence of halogen free materials[1,2]. These so-called HFFR (Halogen Free Fire Retardant) can contain a high amount of Aluminium hydroxide (ATH)or Magnesium hydroxide in order to make them comply with the more and more stringent fire behaviour requirements especially regarding the toxicity and the opacity of the emitted smoke.

However, the action of water (diffusion, location, water uptake...) on highly filled insulation or jacketing for low voltage applications has been sparsely investigated. The ATH filler is used for its well-known fire-retardant properties[3], but ATH is also anhydrophilic filler and when the material absorbs water, it loses some of its insulating properties (insulation resistance, breakdown...).Hsu et al.[4,5] have studied for example the evolution of the functional properties of low and medium voltage cables. They pointed out that the moisture-related degradation during extended immersion in water provokes a decrease of the insulation resistance and an increase of capacitance (leakage current). They also demonstrated that physical ageing (swelling, fillers de-cohesion...) leads to the formation of voids, responsible for new moisture diffusion paths but no attention was paid to the water diffusion mechanisms nor to the contribution of fillers on the latter.

In composite materials, fillers are linked to the polymer matrix by connections/interactions that are established at the interfaces. The material properties (mechanical, electrical…) are tightly related to the stability of these links. It is well known that the interface between the polymer and the filler play a key role in the resulting properties of the composite. The most common methods to identify the quality of the interfaces are based on the observation of the mechanical properties of the material. Several studies focus on the Payne and Mullins

effects[6,7] for example to evidence the influence of the interfaces through the analysis of the mechanical properties under cyclic or growing strain amplitudes. Another approach consists in probing the free volumes of the composite using techniques like the Positron Annihilation Spectroscopy (PALS)[8] or the Nuclear Magnetic Resonance Spectroscopy (NMR)[9]. The work of Valentin et al.[10] especially presents interesting correlations between NMR and swelling techniques to elucidate these interfaces. They focus on filled rubbers to determine if fillers are covalently bounded with the polymer or not. We finally notice that authors also used dielectric spectroscopy[11] using water as a probe to evidence the interfaces.

The purpose of this article is to show that with the thermoporosimetry technique, it is possible to study the morphology of filled polymers. The use of this technique with water molecule as a probe allows studying the distribution and the location of the absorbed water inside the material. We attempt, especially, to show that in these ATH filled polymers, water concentrates within the polymer/filler interfaces. With cyclohexane as a probe, this technique is used to study the morphology of the polymer matrix far away from these interfaces.

2. Experimental

2.1. Materials

Composite samples were based on a copolymer Ethylene-vinyl Acetate (EVA) with AluminiumTriHydroxides ($Al(OH)_3$) denoted ATH. The EVA copolymer was supplied by ExxonMobil Chemical, grade Escorene®UL00328, with the following properties: vinyl acetate co-monomer content = 27% by weight (Scheme 1), density = 0.951 $g.cm^{-3}$, melting point = 73°C. Commercially available AluminiumTriHydroxides (ATH, density 2.4 $g.cm^{-3}$) were supplied by Nabaltec. Thetextural properties of ATH fillers aresummarized in Table1. The Apyral 40VS1 is an Apyral 40CD with a proprietary vinyl silane treatment from Nabaltec.

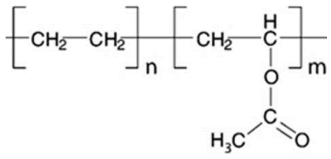

Scheme 1. EVA chemical structure (m = 0.27)

Table 1. Textural properties of the ATH fillers. D_{50} = median diameter, SSA (BET) = Specific Surface Area obtained from the gas sorption method (BET).

Filler name	Surface treatment	Type	D_{50} [µm]	SSA [$m^2.g^{-1}$]
Apyral 1E	No	Coarse grained	45	0.2
Ap. 40CD	No	Average size	1.3	3.5
Ap. 40VS1	Vinyl silane	Treated Average size	1.5	3.5
Ap.200SM	No	Fine grained	0.4	15

2.2. Processing of composites

All the formulations were silanecrosslinked[12,13]. Thus the silane grafting of EVA was performed thanks to a mix of Vinyl-TriMethOxysilane (VTMO) and DiCumyl Peroxide (DCP) supplied by Evonikand using a twin screw extruder with temperatures ranging from 170°C to 200°C. The screw speed was 200 rpm for a material output of 8 $kg.h^{-1}$.

The resulting grafted EVA was then compounded with ATH fillers in an internal mixer Brabender 300 cm^3 at initial temperature 120°C with rotors speed 20 rpm. Fillers were incorporated after 2 minutes and mixed for an average time comprise between 10 to 12 minutes. Mixing was finalized in an external mixer at 90°C and sheets were produced. These sheets were pressed at 180°C during 2 minutes to obtain 1 mm thick-plates. Crosslinking was achieved placing the samples in water at 65°C for 48 hours. Table 2 summarizes the studied formulations.

Table 2. Composition of EVA/ATH composites.

	ATH content for the EVA/ATH composites (% wt)			
Name	Average SizeAp40CD	Coarse GrainedAp1E	Fine GrainedAp200SM	Treated Average SizeAp40VS1
REF	0.0			
AV20.0	20.0			
↓	**↓**			
AV66.7	66.7			
CG50.0		50.0		
FG50.0			50.0	
TA50.0				50.0

The average size ATH filler (Ap40CD) is used to study several filler contents from 20 to 66.7 % in weight which respectively corresponds to 8.7 to 43.3% in volume. To test the influence of the Specific Surface Area (SSA), a filler content of 50.0% wt (27.7% in volume) was chosen to prepare composites with different ATH particles.

2.3. Thermoporosimetry

Thermoporosimetry is a particular application of DSC. The basic principle of thermoporosimetryhas been widely reported in the literature[14-20]. Basically, when a liquid is confined inside a small volume, its crystallization temperature decreases depending on the size of the space in which the liquid is trapped. The relationship between the decrease of crystallization temperature ($\Delta T = T_p - T_0$) and the pore size (R_p) is given by Gibbs-Thomson equation (Equation 1).

$$\Delta T = T_p - T_0 = \frac{2\sigma_{SL} Cos(\theta) T_0}{\Delta H_m \rho_s R_p} \approx \frac{k}{\Delta H_m R_p} \quad (1)$$

whereT_p is the melting temperature of a liquid confined in a pore of radius R_p, T_0 is the normal melting temperature of the liquid, σ_{SL} is the surface energy of the solid/liquid interface, θ the contact angle, ΔH_m is the melting enthalpy, $\rho_S$the density of the solid and *k* a constant.

To establish the relationship between R_p and ΔT and transform the crystallization thermogram of the confined liquid into pore sizes distributions, it is necessary to perform a calibration[21,22]using a set of mesoporous silica whose pore size distributions are known and has been determined by alternative method (usually by gas sorption). A calibration with water as a probe was performed with the water used in the study (tap water) to be more accurate. Figure 1 summarizes the obtained results for calibration.

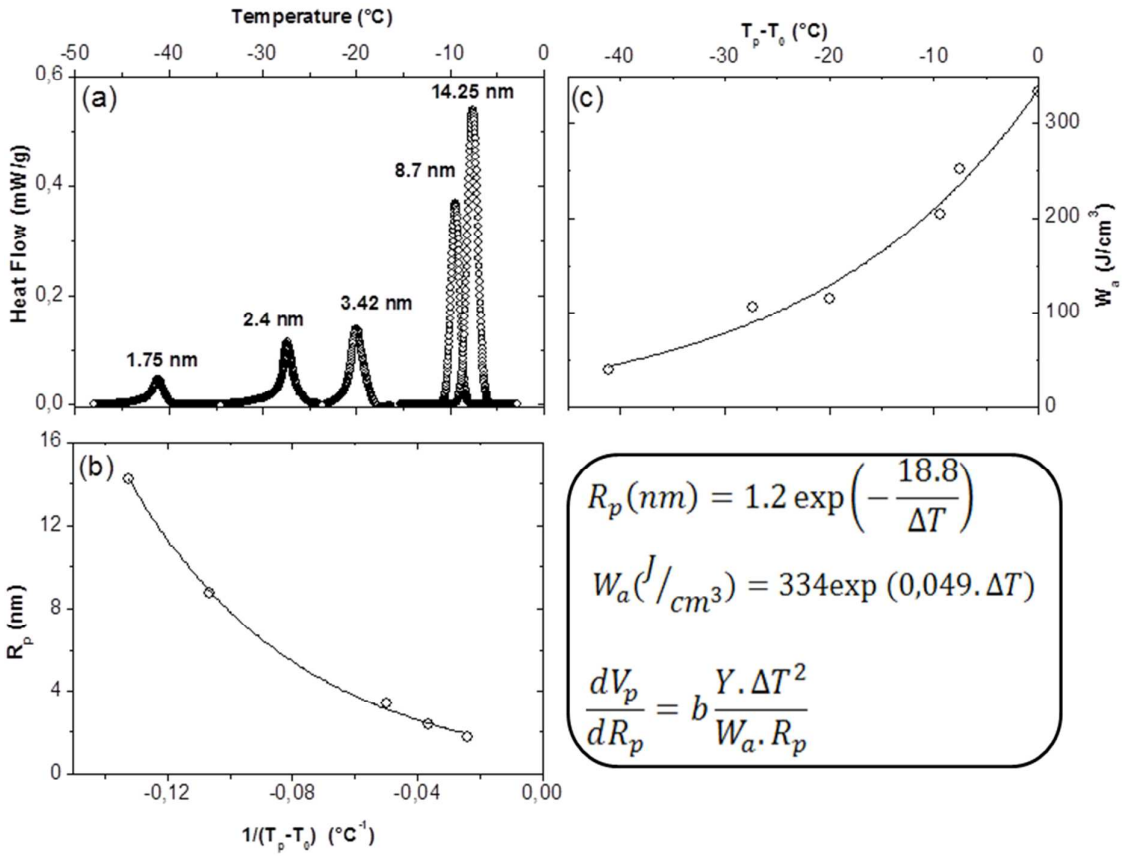

Figure 1. Calibration data with tap water. (a): DSC thermograms of the crystallization of water confined within the standard silica samples with various average pore radii. The cooling rate was of 0.7 °C.min^{-1}. (b): Pore radium as a function of the reverse of the shift of the crystallization temperature (ΔT). (c): The apparent energy of melting (W_a) versus the shift of crystallization (ΔT).

The insert in Figure 1 shows all the numerical relationships obtained from these calibration experiments. W_a is the apparent heat of melting which takes into account the diminution of this energy of the thermal transition along with temperature and also the existence of an adsorbed layer which not crystallizes. "Y" is the ordinate of the DSC thermogram representing the heat flow and "b" is a proportionality factor. These relationships allow transforming of the DSC thermograms of crystallization of confined water into pore size distributions or volume size distributions in which water is confined.

Thermoporosimetrywith cyclohexane, water or both as molecule probes uses a classical temperature program which consists in a cooling from 5 to -60°C at 0.7°C.min^{-1}. An air flow of 40 mL.min^{-1} was maintained in the oven during all the experiment. Swelling in water is achieved after the water uptake experiment (plateau of the diffusion curve). Cyclohexane is known as a good swelling solvent[23] of the crosslinked EVA and swelling is reached after 48 hours at room temperature. For cyclohexane, the conversion of the crystallization thermogram of the confined liquid into pore sizes distributions was performed using the equations published in a previous work[24].

A specific program was used for the thermoporosimetry with drying steps experiment which allows to observe the progressive desorption of the confined solvent and thus to estimate the size of the un-swelled mesh. Successive cooling programs were performed including drying periods between each cooling. Drying was carried out within the DSC furnace. After each drying period, the amount of confined water remaining inside the material was measured by DSCfollowing a temperature program described in Figure 2.

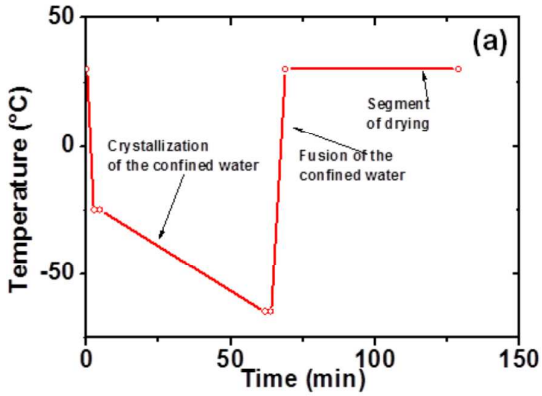

Figure 2. Temperature program managed using DSC for the protocol 'thermoporosimetry with drying steps'. Dry air flow of 40 mL.min^{-1}.

2.4. Other characterization techniques

Dynamic mechanical analyses were performed with a DMA 2980 from TA instruments. The sheets were tested in tensile mode from -30 to 150°C with a heating rate of 3°C.min^{-1}. Strain frequency was fixed at 1Hz and deformation at 0.1%.

Surface analysis of the materials wereperformed using Scanning Electron Microscope (SEM), JSM 6700F from JEOL Company. The abraded then polished surface of the specimens have been sputter-coated with a conductive layer (9 nm - Au/Pd) and all images were made under high vacuum using backscattered electron (WD=15mm, 20 kV, 13A).

Water uptakes were performed in tap water at 90°C. Test specimens of approximately 60×10×1 mm^3 were cut from moulded plates. Before the experience, samples were conditioned in a dessicator to avoid moisture absorption prior to testing. Gravimetric measurements were performed by removing the samples from a water bath held at a constant temperature of 90°C, rapidly removing excess surface water using an absorbent paper and weighting using an electronic balance. The measurements were managed with an accuracy of ± 0.001 g and the presented data are an average value of three samples. The time required to weight the sample was typically less than 2 minutes which was assumed to be sufficiently short not to influence the measured values. The classical expression for modelling a Fickian diffusion from Crank[25] is recalled in Equation 2.

$$\frac{M}{M_\infty} = 1 - \frac{8}{\pi^2}\sum_{n=0}^{\infty}\frac{1}{(2n+1)}\exp\left[-\left(\frac{Dt}{h^2}\right)\pi^2(2n+1)^2\right] \quad (2)$$

Where h is the thickness of the specimen, D the coefficient of diffusion and M_∞ equilibrium moisture content. For $Dt/h^2 > 0.05$, Eq. (2) can be reduced to Eq. (3):

$$\frac{M}{M_\infty} = 1 - \frac{8}{\pi}\exp\left[-\left(\frac{Dt}{h^2}\right)\pi^2\right] \quad (3)$$

For $Dt/h^2 < 0.05$, Eq. (2) reduces to Eq. (4):

$$\frac{M}{M_\infty} = \frac{4}{\sqrt{\pi}}\left(\frac{Dt}{h^2}\right)^{1/2} \quad (4)$$

M is the moisture content defined as the moisture per unit of volume of the specimen and is expressed as the percentage of its dry weight.

TGA/humidity coupling consists in a microbalance coupled with a humidity generator. The microbalance is used from a Mettler TGA/DSC1 with 0,1µg resolution. The humidity generator is a HumiSys model. This coupling device allows working with a relative humidity ranging from 0 up to 90 % and a temperature from 30 to 90°C.

3. Results and discussion

3.1. Characterization of the composite morphology

3.1.1. Scanning Electron Microscopy (SEM)

The EVA/ATH composite samples were first characterizedby SEM using backscattered electrons (Figure 3) to observe the ATH particle dispersion in EVA depending on the particle size, the specific surface area and the surface treatment.

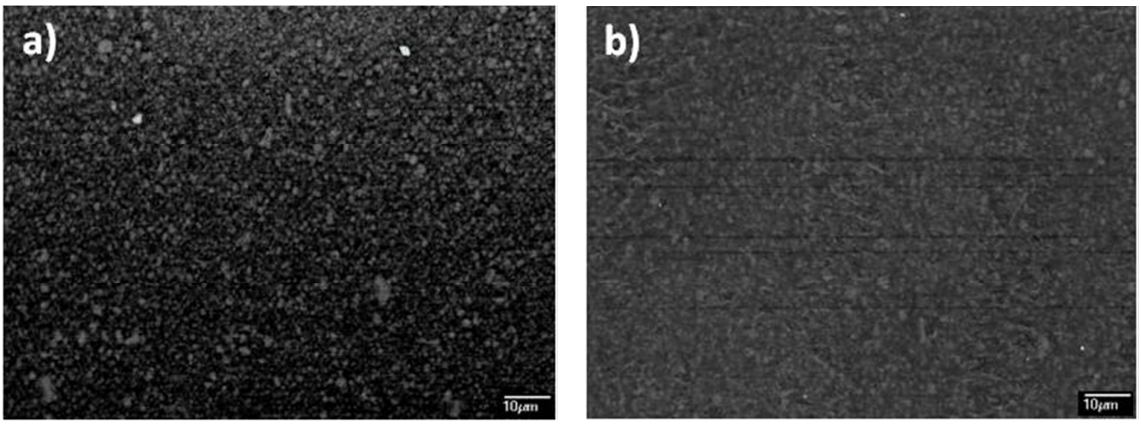

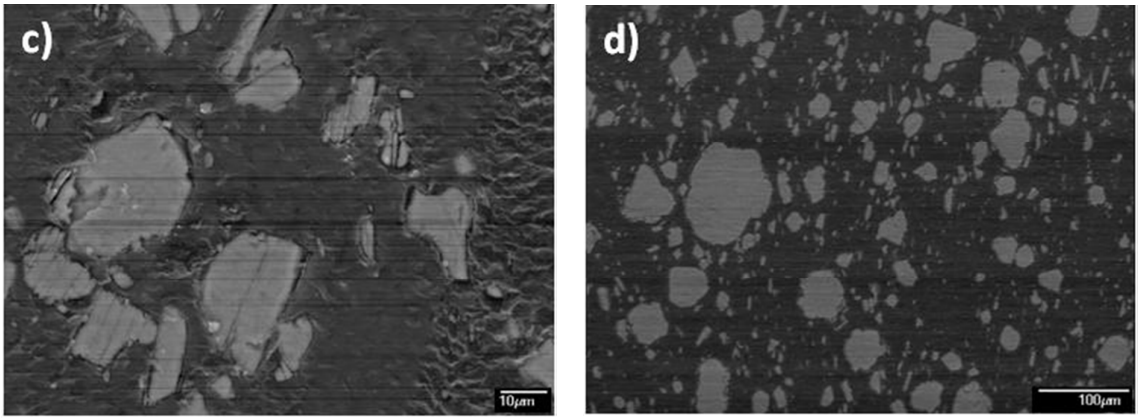

Figure 3.SEM (Backscattered electron) analysis of three EVA/ATH composites at 50% filler loading. A)EVA filled with average size ATH (AV50.0). b)EVA filled with treated average size ATH (TA50.0). c) EVA filled with coarse grained ATH (CG50.0). d) EVA/ATH (CG50.0) at lower magnification.

Figures 3a and 3b are respectively relative to the samples with 50% in weight of ATH (average size and treated average size ATH), which corresponds to 28.2% of filler in volume. ATH fillers appear as white, almost spherical particles and are well dispersed in the polymeric matrix for both cases, with no visible difference (except the contrast).Figure 3a shows that the ATHsize is close to that given in the informationfrom the supplier with an average diameter of 1.3μm. Concerning the coarse grained ATH (Fig. 3c), the particle size is also consistent with the given 50μm. A SEM image at lower magnification for this EVA/ATH sample is given in Figure 3d for a better observation of the ATH distribution within the EVA matrix. For this filler, the polymer-filler interface is clearly visible. No picture of EVA filled with fine grained ATH is given due to the SEM technique which is not efficient to observe particles with an average diameter of 400nm.

3.1.2. Dynamic Mechanical Analysis (DMA)

The composites were characterized by DMA in term of storage modulus versus temperature in the range -20 to 140°C. The goal was to study the impact of ATH on the mechanical properties of the materials in comparison to pristine EVA. Figure 4 shows the effect of ATH content with particles of average size (Fig. 4a) and the influence of particle specific surface area (at 50%wt loading) (Fig. 4b).

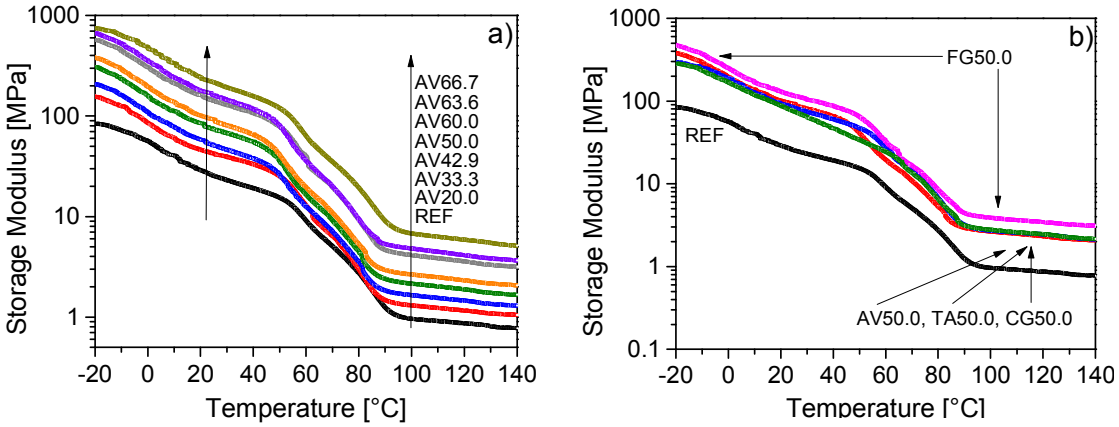

Figure 4. Storage modulus versus temperature for the studied composites: a)Influence of the filler content for EVA filled with average size ATH, b) Influence of the filler SSA for EVA filled at 50% in weight.

One can observe first that the pristine EVA (REF) has a first loss of modulus from -20 to around 50°C (Tg is close to -40 for EVA 27%). The second and third losses of modulus above 50°C and 90°C respectively correspond to the melting of the crystallites (melting peak at 73°C in the literature) and to the rubbery plateau given as the polymer is crosslinked. As observed at 90°C, the temperature of the water for the immersion tests, EVA is in its rubbery state.Regarding the influence of the filler content (Fig. 4a), it is observed that the filler acts as a reinforcement for the modulus at room temperature (before the melting) and for the modulus on the rubbery plateau (after the melting). An increase of almost one decade is obtained from the pristine EVA to the highly filled compound (AV66.7). The influence of the specific surface is less contrasted (Fig. 4b), if a higher reinforcement is obtained for the fine grained

ATH (FG50.0), the effect of the three other fillers (average, treated average and coarse grained) is very similar in terms of storage modulus enhancement on the whole temperature range.

3.1.3. Thermoporosimetry using cyclohexane as a probe

To characterize the polymer network of the composites, thermoporosimetry with cyclohexane as a probe was performed. As for the DMA experiments, Figure 5 presents the influence of the filler content (Fig. 5a) and the influence of the specific surface area (Fig. 5b) on the mesh size distributions.

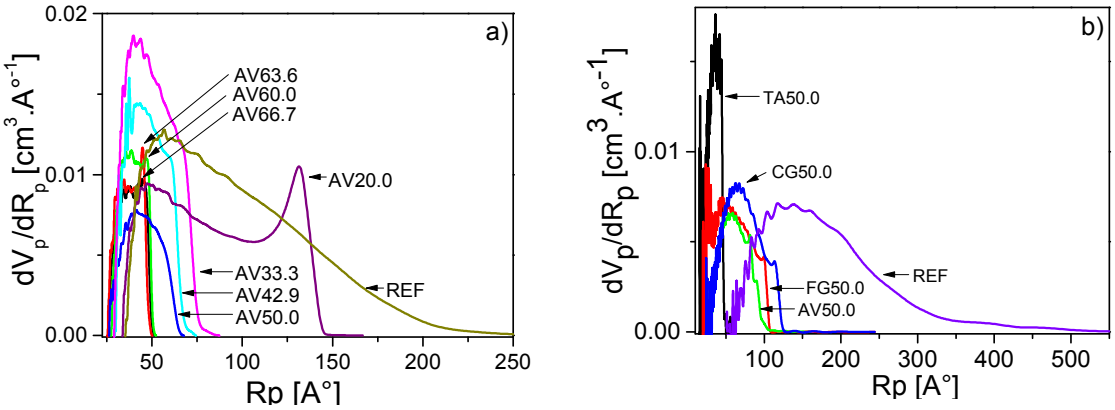

Figure 5. Mesh size distributions of the volumes confining cyclohexane for EVA/ATH composites: a)Influence of the filler content for EVA filled with average size ATH, b) Influence of the filler SSA for EVA filled at 50% in weight.

As observed in both figures, pristine EVA (i.e. the unfilled crosslinked EVA = REF) presents a wide distribution of volumes that can confine cyclohexane from around 50 Å to 25-45 nm. As recalled in the experimental part, EVA wascrosslinked using silane and it is known[26] that the network obtained using this crosslinking methodhas a lower crosslinking density in comparison with peroxide cured one. It is however interesting to note that the mesh size is not a Gaussian repartition with obtained values centred at around 75-100 Å. Concerning the effect

of the filler content (Fig. 5a), one can see that fillers reduce the mesh size. This is observed on both the mesh size value and the width at half maximum, which both decrease when increasing the content of fillers. For the highly filled compound (AV66.7), the mesh size is comprised between 25 and 50 Å. It is well known[27] that the silanol functions condensate to form crosslinking, but these functions can also react with the hydroxyl groups at the surface of the filler, as shown in Figure 6. The filler can act as crosslinking agent because of these covalent bonds and can also contribute tothe mechanical reinforcement leading to the decrease in the swelling of the material (physical effect). Discriminating both these effects is rather difficult. However, it can be noticed that the sample with the lowest rate of ATH (AV20.0) shows a mesh sizes distribution different from that of the other samples. It is very likely that this difference is due to a lack of homogeneity in the distribution of fillers particles within the polymeric matrix.

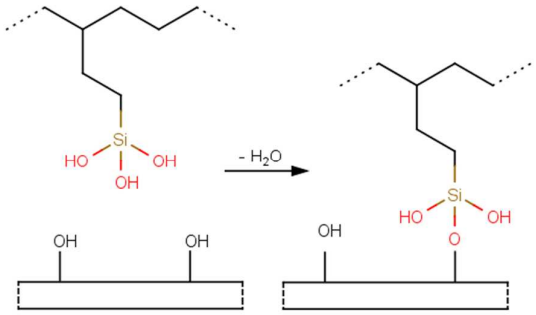

Figure 6. Condensation reaction between an available silanol function of the grafted polymer and the filler surface.

Regarding the effect of the filler SSA (Fig. 5b), the effect is similar. The smallest values of mesh size are obtained for the treated filler. However, one can notice that the surface treatment seems to influence the apparent densification of the network.

To complete the network characterization, the amount of the confined cyclohexane (area under the curve) measured by thermoporosimetrywas plotted versus the filler content and the filler SSA, as shown in Figure 7.

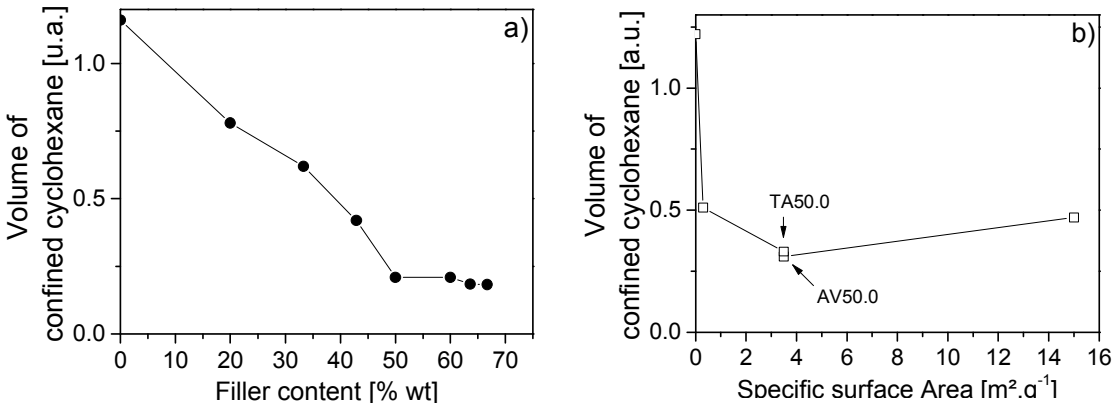

Figure 7. Volume of confined cyclohexane obtained from the measured area under the curves of thermoporosimetry: a)versus the filler content, b) versus the SSA.

Figure 7a shows that the volume of confined cyclohexane decreases versus the filler content until a value around 50% is reached. This decrease is in accordance with the apparent densification of the network (Fig. 5a) leading to the reduction of the swelling and thus a reduction in the solvent uptake. For loading higher than 50%, this effect is no longer observed and it would mean that a similar network is then obtained for filler contents over 50 wt%. It could be due to the beginning of a filler agglomeration which reduces the accessible filler surface by the polymer chains. Regarding the influence of the SSA (Fig. 7b), adding ATH filler at 50% leads to a reduction of the cyclohexane uptake but no significant influence of SSA is observed. As observed in Figure 3, microscopy is not pertinent to characterize the filler dispersion for these samples where one can found very high rate of fine fillers. However, the filler agglomeration is invoked because we know from several studies[28-29] that these composite systems could reach a percolation concentration depending on the filler size and shape, concentration. From these studies, we know that rising the filler concentration, agglomerates of the filler particles begin to form. In these agglomerates, the filler particles are in contact leading to filler networks, polymer occlusion.

3.2. Characterization of polymer-filler interfaces using water as a probe

3.2.1. Water uptake by ATG

Water adsorption onto the ATH filler particles (before compounding with the EVA) was characterized. The experiments were conducted using an ATG/humidity coupling, which allows measuring the water uptake by a sample in a given relative humidity (RH). Figure 8shows the isotherms obtained during the water saturation of the pure ATH fillers, corresponding to water adsorbed onto the surface of the filler particles.

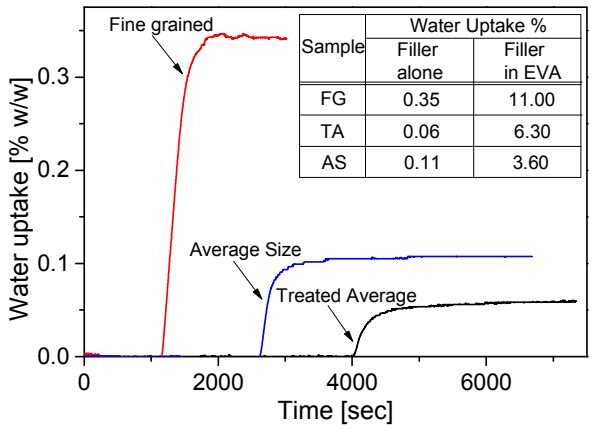

Sample	Water Uptake %	
	Filler alone	Filler in EVA
FG	0.35	11.00
TA	0.06	6.30
AS	0.11	3.60

Figure 8. Water uptake of ATH fillers measured by the ATG/humidity coupling (HR=90% and T=30°C). Insert: comparison between the water uptake of the filler and of the corresponding filled EVA (containing the same filler at 50% wt).

It can be observed in Figure 8 that the fine grained filler adsorbed much more water than the average size and the treated one. This indicates that the SSA plays a key role on water adsorption. In order to comparethe amount of adsorbed water onto the ATH particles with the same ATH particles but in the corresponding composite (insert of Figure 8) and the water absorbed by the filled polymers, the amount of absorbed water(performed by a double weighing, before and after soaking)was expressed by the mass unit of filler (taking into account that the filler content is 50%). As shown below (Fig.10), the filler alone absorbs no water. The values shown in the insert Fig. 8 indicate then that the percentages of absorbed

water in composites are much more important than the percentages of the adsorbed water onto the filler surface.

3.2.2. Water uptake by gravimetry

Water uptake at 90°C by EVA/ATH samples was characterised by gravimetry. Long time immersions were required and the gravimetric curves are presented in Figure 9. A Fickian treatment of the experimental data was performed and is shown inFigure 9b where normalised Mt/M_∞ versus the square root of time is plotted.

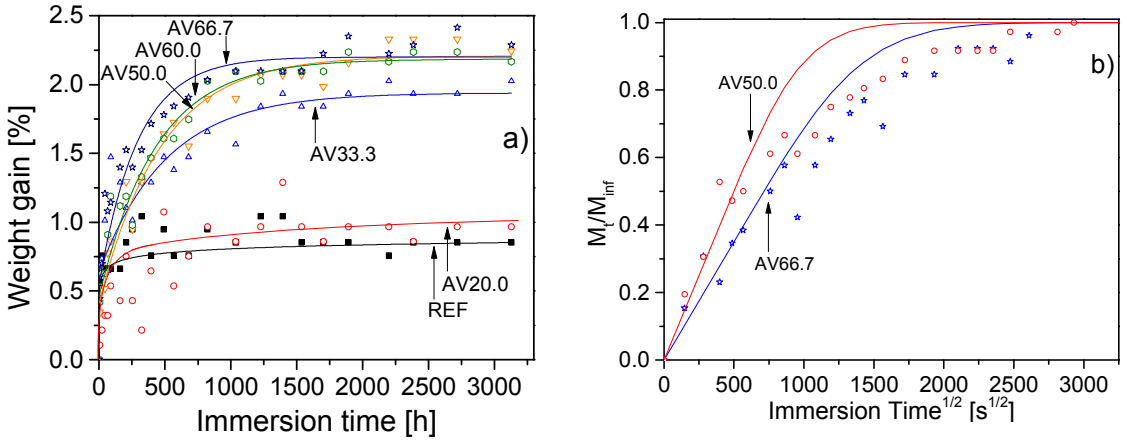

Figure 9.a) Weight gain versus immersion time at 90°C for different filler contents. b) Application of the Fickian model (lines) to gravimetric data (dots) for 2 filler contents (50 and 66.7%).

Figure 9a shows that ATH at loading higher than 20% leadsto a notable increase in the water uptake at 90°C. Whereas the water uptake of unfilled EVA remains below 1% weight gain, it reaches more than 2% for samples with 33% or moreATH filler. Additionally, one observes that for filler loading above 33%, the weight gain at infinite does not depend on the filler content.Regarding these curves, a Fickian treatment (continuous lines) of the data was proposed in Fig 9b. The mismatch observed between the experimental data and the Fickian

fits is likely to reveal that the water diffusion in the filled materials is a non-Fickian process. Despite this mismatch, the coefficient of diffusion was calculated using Equation 4 (below $M_t/M_{inf} < 0.5$, the experimental data are close with the Fickian model).One found for the unfilled EVA (REF) at 90°C a coefficient of around 4.10^{-12} $m^2.s^{-1}$, for the AV50.0 a value of around 1.10^{-13} $m^2.s^{-1}$ and for the AV66.7 a value of around 2.10^{-13} $m^2.s^{-1}$. For $M_t/M_{inf} > 0.5$, the diffusion is slower than the model. Thus, a dual diffusion phenomenon (Langmuir/Carter and Kibler modelisation[30-32]) with a slower second diffusion speed is more realistic to describe the diffusion in the composites. One can explain this behaviour because of the high hygroscopicity of ATH (polar surface), i.e. the water molecules diffusion is reduced in a second step because of the chemical affinity with the filler surface through hydrogen bonding.

3.2.3. Thermoporosimetry with water: influence of the filler content

In a first time, thermoporosimetry analysis with water was performed on one composite sample labeled AV50.0 (EVA filled with 50% of average-size ATH) and on the pure filler (also the average-size). Figure 10 shows the DSC thermogram corresponding to the cooling of the samplesAV50.0and the pure average-size filler (Apyral40CD), both waterlogged.

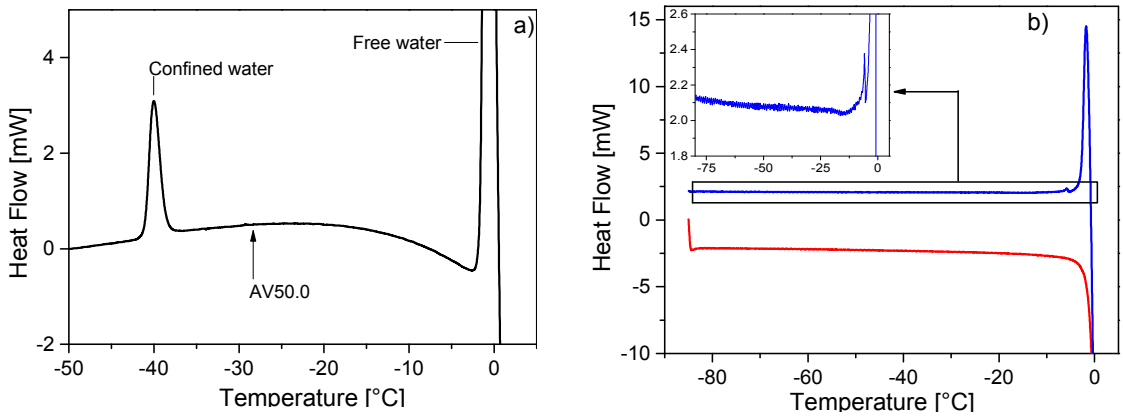

Figure 10.a) DSC thermogram of crystallization of the water soaked sample AV50.0,b) DSC thermogram of the Apyral 40CD filler soaked in water. The insert shows the zoom of the base line.

DSC thermogram of Figure 10a shows two peaks: the peak around 0 °C is attributed to free water, which was in excess and remained at the outer surface of the sample, the peak around -40°Cthat corresponds to the confined water. According to the calibration curves (Fig. 1), this water is confined inside a pore volume having 1.9 nm as characteristic dimension. This means that this EVA/ATH sample filled at 50% wtcontains water confined in small pores in a diameter range of 2 nm. Figure 10b shows the DSC thermogram obtained during the cooling (blue line) of the average-size ATH waterlogged. As the magnification of this graph shows, there is no crystallization peak other than that of the free water appearing at 0°C. So, it confirms that the water previously attributed to the confined one that wasobserved in the composite,is not confined inside the ATH filler itself.

The influence of the ATH content on the amount of confined water was then studied. Figure 11apresents the mesh size distributions of the volumes confining water in EVA/ATHcomposites with increasing filler loadings from 0 to 66.7% wt.Analyzed samples were taken out from water at 90°C after 3000 hours (water uptake plateau – see Figure 5). The amount of confined water (area under the curves of thermoporosimetry)versus the filler content was also given (Fig. 11b).

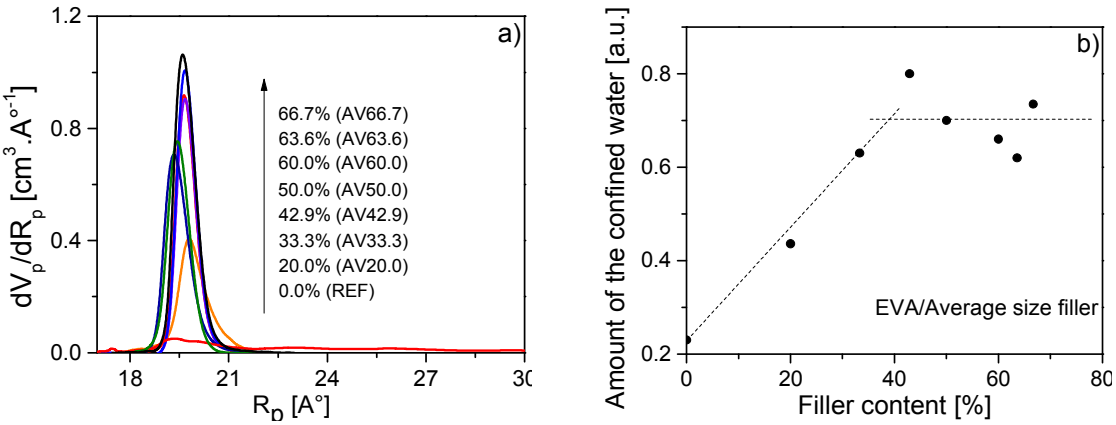

Figure 11.a): Mesh size distributions of the volumes confining water for EVA/ATH composites with increasing filler content (from 0 to 66.7%), b) Amount of confined water versus the filler content in EVA/ATH (average size filler).

The DSC thermograms obtained from thermoporosimetry measurement were converted into the mesh size distributions shown in Figure 11. The volumes confining water for all the EVA/ATH composites remain in a same range of 2 nm. The areas under the peak of these mesh size distributions are proportional to the amount of trapped water. As observed in Figure 11b, the amount of confined water increases with the filler content up to 40% in weight (≈ 23% in volume). Beyond this filler content, the amount of confined water remains approximately constant. It is very likely that this limit (around 40%wt) corresponds to a threshold regarding the fillers dispersion. Below this filler content, the fillers would be dispersed without agglomerates and their whole surface would be accessible to water. Beyond this content, the fillers begin to form aggregates,andincreasing their amount does not increase the total surface accessible to water molecules.This is in good accordance with the results reported above in Figure 9, which indicated that the water uptake no longer increased for filler content up to 33.3% in weight. However, thermoporosimetry gives more information than gravimetry because it permits the distribution of volumes confining the water to be characterised.

3.2.3. Thermoporosimetry with water: influence of SSA

Thermoporosimetry analysis was then performed on fully water soaked composites with 50% of ATH but with different specific surface area (SSA).Figure 12 shows the DSC thermogramsand the corresponding results.

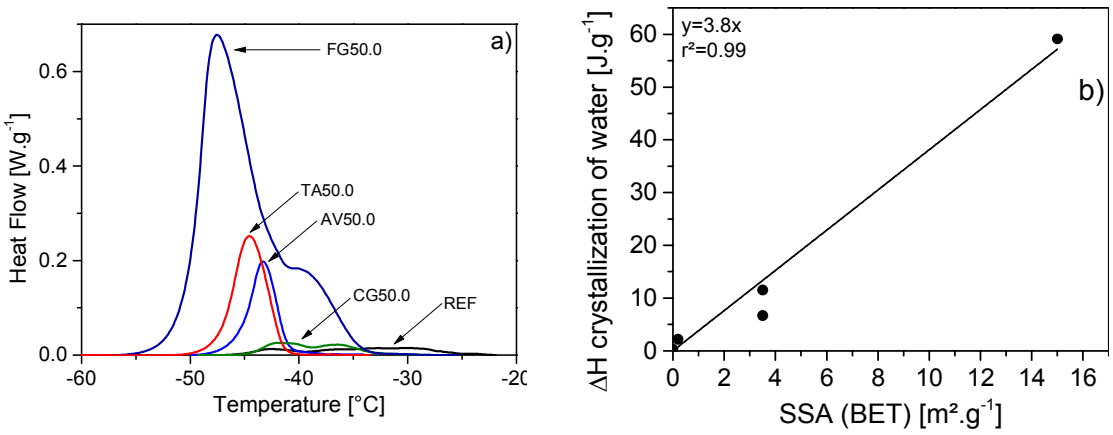

Figure 12.a)DSC thermograms of the crystallization of the confined water within EVA/ATH (50%wt) composites with ATH of different SSA, b) Heat of crystallization (ΔH) of confined water versus SSA (BET).

Figure 12ashows that the crystallization peak of confined water in the different composite samples is between -50°C and -40°C. ΔH crystallization of confined water ($J.g^{-1}$) was calculated by dividing the peak area by the polymer mass of each analyzed sample. Normalized values are then plotted versus the specific surface area of the ATH filler measured using BET (SSA) as presented in Figure 12b. One can observe that the larger is the SSA of the filler, the larger is the increase of the energy of crystallization. Figure 12b shows that the crystallization energy is proportional to the amount of confined water. The intercept of the linear extrapolation was fixed at 0 even if the experimental ΔH value for the unfilled EVA was found at 0.34 $J.g^{-1}$.Thislinear relationship would give a first indication that the confined water is localized at the polymer-fillers interfaces. These results reflect the fact that water is confined inside a polymeric network attached onto the surface of the fillers.

3.2.4. Structure of the polymer-filler interfaces

To complete the characterization of the structure of the polymer-filler interfaces, two complementary experiments were conducted on the composites. The first one consists in drying a sample within the DSC furnace andthen measuring the amount of confined water remaining inside the material by DSC (Fig. 13). The second one consists in the simultaneous use of two molecular probes to investigate the morphology of the polymer or the composites (Fig. 14). The two specific protocols were fully described in the experimental part.

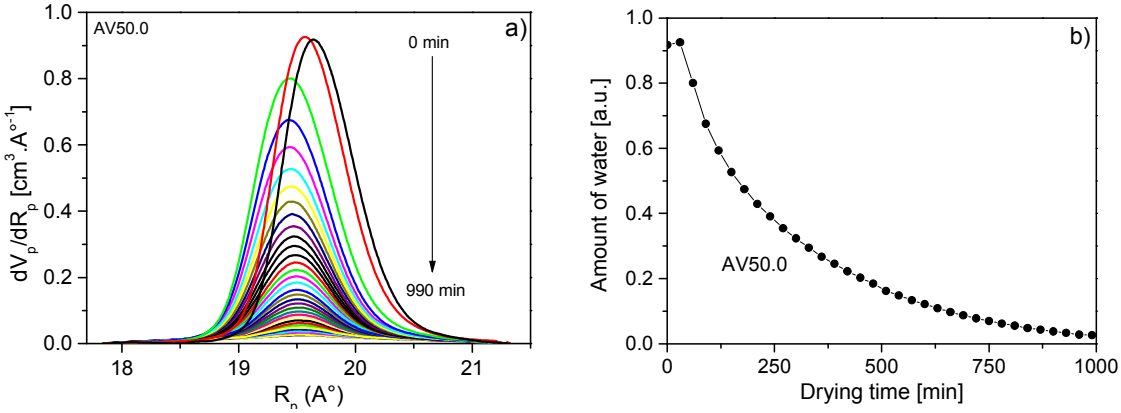

Figure 13. Drying experiments of an EVA/ATH composite sample (AV50.0).a) Evolution of the mesh size distributions obtained from DSC thermograms during drying, b) Amount of confined water as a function of drying time.

Thetime required to dry the sample wasranging from 0 to 990 minutes, which allowed a total drying. As observed, there is a gradual diminution of the area under the curves, which reflects a gradual evaporation of the confined water. A first remark can be made about the distributions shown in Figure 13: except the first two mesh size distributions, all others are centered on a single value of mesh size (19.5 Å). Desorption of water is not accompanied by a deflation of the polymer which indicates that water does not swell the polymer and water molecules occupy spaces that were free. The two first distributions havealready been observed[33,34]and it has been recently interpreted as due to the change in tensile pressure acting on the pore condensate[35].

Figure 13b shows the variation of the amount of confined water as a function of drying time. This curve was obtained by measuring areas under the crystallization peaks, which are proportional to the amount of the crystallized water. It represents the desorption isotherm of water at 30°C.Using the same protocol (see Equ.4), the coefficient of diffusivity is measured for this sample and one found a value of around 1.10^{-11} $m^2.s^{-1}$. This coefficient corresponds to the water desorption in the sample AV50.0 at 30°C. Even if it can't be directly compared with the previous value of 1.10^{-13} $m^2.s^{-1}$found for the sorption at 90°C, it is important to notice that the desorption is faster in comparison with the sorption in the composites. This difference between the sorption and desorption may also be observed by comparing the times to the two phenomena to reach 50% of their optimal value. In Figure 9b (sorption), this time is 250 000 seconds (4166 minutes), whereas it is only 7800 seconds (130 minutes) on Figure 13b (desorption). The explanation for this large difference could be sought in the difference between the diffusion conditions, i.e. the sorption is carried out by soaking the sample in stagnant liquid water while desorption is achieved by passing a dry air stream on the sample.

To characterize the morphology of the EVA composites, at two different scales, thermoporosimetry analysis was then performed by the simultaneous use of two molecule-probes, water and cyclohexane. We have shown above, that water does not swell crosslinked EVA but accumulated at the EVA/ATH interface where it is confined. A sample of EVA filled with fine grained ATH and soaked in water at 90°C for 3000 hours was then soaked in cyclohexane to achieve the swelling of the polymer network by cyclohexane. This sample was subsequently analyzed bythermoporosimetry. The results obtained are gathered in Figure 14.

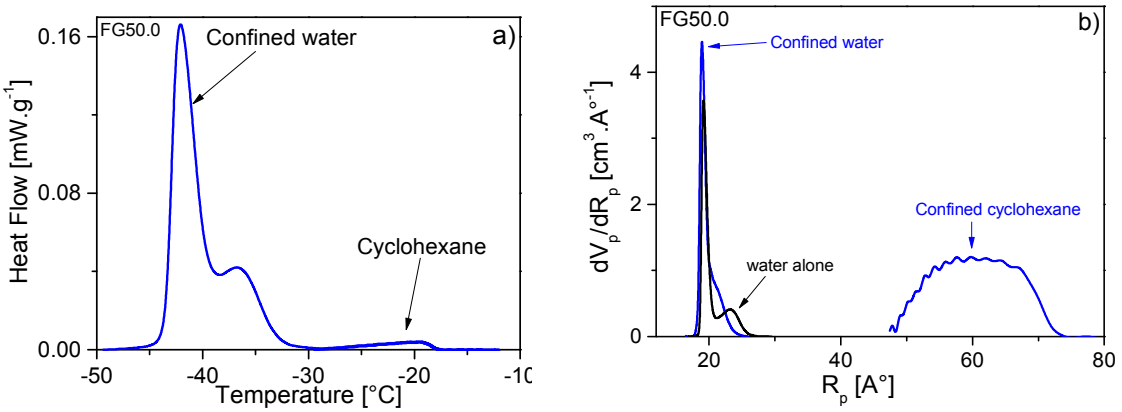

Figure 14. Simultaneous use of water and cyclohexane to investigate the morphology of the material.a) DSC thermogram of EVA/ATH composite (50%) swollen by cyclohexane after 3000h soaking in water, b) corresponding mesh size distribution (blue line) and the mesh size distribution of the same composite soaked only in water (black line).

The DSC thermogram of the two confined liquids presents two main peaks around -20°C for cyclohexane and around -40°C for water (as shown in Figure 12). This thermogram was transformed into mesh size distribution as presented in Figure 14b. Two populations of meshes were obtained. The first one, centered at about 6 nm, corresponds to the network of the crosslinked EVA swollen with cyclohexane (see Fig.5). The second one, centered at around 2 nm, is related to the confined water. By superimposing the mesh sizes distributions of the same composite sample swollen either in water alone or with both solvents, we observe that this second population is related to the water confined at the polymer-filler interface. So, it seems that the water located at the polymer-filler interfaces is not influenced by the presence of cyclohexane. This organic solvent, having no particular affinity with the ATH fillers, is located essentially in the polymeric part, away from the interfaces.

It also can be observed the double distribution exhibited by the water signal provide from this sample. This double distribution was little affected by the absorption of cyclohexane by the sample. It denotes the existence of two populations of meshes present at the polymer/fillers

interface and having very close sizes. It can be explained by the heterogeneity of the distribution of fillers or crosslinking agents.

4. Conclusion

In this article we have shown that the water molecule can be advantageously used to probe the interface between a polymer matrix such as EVA and hydrophilic filler as ATH. With thermoporosimetry technique, we have shown that the water absorbed by the material is concentrated at the interfaces. This conclusion was supported by several observations including, in particular, the quasi-proportionality relationship between the amount of absorbed water and the total specific area of the filler. Furthermore, we have shown that the absorbed water is confined in the voids (interstices) whose mean diameters are between 1.9 and 2 nm. Upon drying the polymer, these interstices not diminish in volume which proves that the water does not cause the swelling of the material.

We have also shown that the use of a hydrocarbon (cyclohexane) as a swelling solvent can probe the morphology of the polymer matrix away from the interface filler/polymer. The simultaneous use of the two probes (water and cyclohexane) confirmed that the water was concentratedat the interfaces while cyclohexane was found within the polymer matrix.

References

1G. Camino,L. Costa,*Polym.Degrad.Stab.,*1988, **20**, 271-294.

2F. Carpentier,S. Bourbigot, M. Le Bras,R.Delobel,M. Foulon,*Polym.Degrad.Stab*.,2000,**69**, 83-92.

3A. Witkowski,AA. Stec,T. Richard Hull,*Polym.Degrad.Stab.,*2012,**97**, 2231-2240.

4YT.Hsu,KS. Chang-Liao,TK. Wang,CT. Kuo,*Polym.Degrad.Stab.,*2006, **91**, 2357-2364.

5YT.Hsu,KS. Chang-Liao, TK. Wang,CT. Kuo,*Polym.Degrad.Stab.,* 2007,**92**, 1297-1303.

6J. Kalfus,J. Jancar,*Polym.Compos.,* 2007,**28**, 725-732.

7J. Diani,B. Fayolle,P. Gilormini,*Europ.Polym. J.,* 2009,**45**, 601-612.

8SJ. Lue,DT. Lee,JY. Chen,CH. Chiu,CC. Hu,YC. Jean,JY. Lai,*J.Membr.Sci.,*2008,**325**, 831-839.

9B. Gabrielle,C. Lorthioir, F. Lauprêtre,*J. Phys.Chem. B,* 2011,**115**, 12392-12400.

10JL. Valentin,I. Mora-Barrantes,J. Carretero-Gonzalez, MA.Lopez-Manchado, P.Sotta,DR. Long,K. Saalwachter,*Macromolecules,*2010,**43**, 334-346.

11M. Böhning,H. Goering,A. Fritz,KW.Brzezinka,G. Turky,A. Schönhals,B. Schartel,*Macromolecules,*2005,**38**, 2764-2774.

12J. Morshedian,PM. Hoseinpour, *Iran.Polym. J.,*2009,**18**, 103-128.

13K. Sirisinha,S. Chimdist,*Polym. Test.,*2006,**25**, 518-526.

14HK.Christenson,*J.Phys: Condens.Matter.,*2001,**13**, R95.

15J. Dore,*Chem. Phys.,*2000,**258**, 327-347.

16CT. Kresge,ME. Leonowicz,WJ. Roth,JC. Vartuli,JS. Beck,*Nature,*1992,**359**, 710-712.

17JW.Gibbs,*Collected works.* New Haven, CT: Yale University Press, 1928.

18SW. Thomson,*Phil. Mag.,*1871,**42**, 448-452.

19CL. Jackson,GB. McKenna,*J. Chem.Phys*., 1990,**93**, 9002-9011.

20M. Brun,A. Lallemand, JF. Quinson,C. Eyraud,*Thermochim.Acta,*1977,**21**, 59-88.

21N. Billamboz,M. Baba,M. Grivet,JM. Nedelec,*J. Phys. Chem. B,*2004,**108**, 12032-12037.

22N. Bahloul,M. Baba,JM. Nedelec,*J. Phys. Chem. B,*2005,**109**, 16227-16229.

23YX.Bai,JW. Qian,Q. Zhao,ZH. Zhu,P. Zhang,*J.Memb. Sci.,*2007,**299**, 45-53.

24SAE.Boyer, M. Baba,JM.Nedelec,JP. Grolier,*Int. J.Thermophys.,*2008,**29**, 1907-1920.

25J. Crank,*The mathematics of diffusion.* Oxford: Clarendon Press, 1975.

26M. Celina,GA. George,*Polym.Degrad.Stab.,* 1995,**48**, 297-312.

27Y. Xie,CAS. Hill,Z. Xiao,H. Militz,C. Mai,*Composites Part A,* 2010,**41**, 806-819.

28F. Lux, Journal of Materials Science 28 (1993) 285-301

29W. Wang, M. Sain, P.A. Cooper; Composites Science and Technology 66 (2006) 379–386

30HG. Carter,KG. Kibler,*J.Comp. Mater.,* 1978,**12**, 118-31.

31V. La Saponara,*Comp.Struct.,* 2011,**93**, 2180-2195.

32S. Popineau,C. Rondeau-Mouro,C. Sulpice-Gaillet,MER. Shanahan,*Polymer,*2005,**46**, 10733-10740.

33A. Schreiber,I. Ketelsen,GH. Findenegg,*Phys. Chem. Chem. Phys.,*2001,**3**, 1185-1195.

34JM.Nedelec,JP. Grolier,M. Baba,*Phys. Chem. Chem. Phys.,*2008,**10**, 5099-5104.

35C. Schaefer,T. Hofmann,D. Wallacher, P. Huber,K. Knorr, *Phys. Rev. Lett.,*2008,**100**, 175701.